REPORT DOCUMENTATION PAGE

Form Approved OMB NO. 0704-0188

1. REPORT DATE (DD-MM-YYYY)	2. REPORT TYPE	3. DATES COVERED (From - To)
	New Reprint	-

4. TITLE AND SUBTITLE

Superlattice multinanolayered thin films of SiO2/SiO2 + Ge for thermoelectric device applications

5a. CONTRACT NUMBER

W911NF-12-1-0063

5b. GRANT NUMBER

5c. PROGRAM ELEMENT NUMBER

206022

6. AUTHORS

S. Budak, R. Parker, C. Smith, C. Muntele, K. Heidary, R. B. Johnson, D. Ila

5d. PROJECT NUMBER

5e. TASK NUMBER

5f. WORK UNIT NUMBER

7. PERFORMING ORGANIZATION NAMES AND ADDRESSES

Alabama A&M University
Office of Research & Development, Patton Hall
P.O. Box 411 4900 Meridan St.
Normal, AL   35810   -1015

8. PERFORMING ORGANIZATION REPORT NUMBER

9. SPONSORING/MONITORING AGENCY NAME(S) AND ADDRESS(ES)

U.S. Army Research Office
P.O. Box 12211
Research Triangle Park, NC 27709-2211

10. SPONSOR/MONITOR'S ACRONYM(S)

ARO

11. SPONSOR/MONITOR'S REPORT NUMBER(S)

60494-EL-REP.13

12. DISTRIBUTION AVAILIBILITY STATEMENT

Approved for public release; distribution is unlimited.

13. SUPPLEMENTARY NOTES

The views, opinions and/or findings contained in this report are those of the author(s) and should not contrued as an official Department of the Army position, policy or decision, unless so designated by other documentation.

14. ABSTRACT

Thermoelectric generators convert heat to electricity. Effective thermoelectric materials and devices have a low thermal conductivity and a high electrical conductivity. The performance of thermoelectric materials and devices is shown by a dimensionless figure of merit, $ZT = S^2\sigma T/K$, where S is the Seebeck coefficient, sigma is the electrical conductivity, T is the absolute temperature, and K is the thermal conductivity. We have prepared 100 alternating layers of SiO2/SiO2 + Ge superlattice thin films using ion beam–assisted deposition for the

15. SUBJECT TERMS

Ion bombardment, thermoelectric properties, transport properties, multinanolayers, figure of merit

16. SECURITY CLASSIFICATION OF:			17. LIMITATION OF ABSTRACT	15. NUMBER OF PAGES	19a. NAME OF RESPONSIBLE PERSON
a. REPORT	b. ABSTRACT	c. THIS PAGE			Satilmis Budak
UU	UU	UU	UU		19b. TELEPHONE NUMBER
					256-372-5894

Standard Form 298 (Rev 8/98)
Prescribed by ANSI Std. Z39.18

Report Title

Superlattice multinanolayered thin films of SiO2/SiO2 + Ge for thermoelectric device applications

ABSTRACT

Thermoelectric generators convert heat to electricity. Effective thermoelectric materials and devices have a low thermal conductivity and a high electrical conductivity. The performance of thermoelectric materials and devices is shown by a dimensionless figure of merit, $ZT = S^2\sigma T/K$, where S is the Seebeck coefficient, sigma is the electrical conductivity, T is the absolute temperature, and K is the thermal conductivity. We have prepared 100 alternating layers of SiO2/SiO2 + Ge superlattice thin films using ion beam–assisted deposition for the thermoelectric generator device application. The 5 MeV Si ion bombardments were performed using the Center for Irradiation Materials' Pelletron ion beam accelerator to form quantum dots and/or quantum clusters in the multinanolayer superlattice thin films to decrease the cross-plane thermal conductivity and increase the cross-plane Seebeck coefficient and cross-plane electrical conductivity. The thermoelectric and transport properties have been characterized for SiO2/SiO2 + Ge superlattice thin films.

Continuation for Block 13

ARO Report Number   60494.13-EL-REP
Superlattice multinanolayered thin films of SiO2/   ...

Block 13: Supplementary Note
© 2013 . Published in Journal of Intelligent Material Systems and Structures, Vol. Ed. 0 24, (11) (2013), ((11). DoD Components reserve a royalty-free, nonexclusive and irrevocable right to reproduce, publish, or otherwise use the work for Federal purposes, and to authroize others to do so (DODGARS §32.36). The views, opinions and/or findings contained in this report are those of the author(s) and should not be construed as an official Department of the Army position, policy or decision, unless so designated by other documentation.

Approved for public release; distribution is unlimited.

Superlattice multinanolayered thin films of SiO_2/SiO_2 + Ge for thermoelectric device applications

Satilmis Budak[1], Robert Parker[2], Cydale Smith[3], Claudiu Muntele[4], Kaveh Heidary[1], Ralph B Johnson[5] and Daryush Ila[6]

Abstract

Thermoelectric generators convert heat to electricity. Effective thermoelectric materials and devices have a low thermal conductivity and a high electrical conductivity. The performance of thermoelectric materials and devices is shown by a dimensionless figure of merit, $ZT = S^2\sigma T/K$, where S is the Seebeck coefficient, σ is the electrical conductivity, T is the absolute temperature, and K is the thermal conductivity. We have prepared 100 alternating layers of SiO_2/SiO_2 + Ge superlattice thin films using ion beam–assisted deposition for the thermoelectric generator device application. The 5 MeV Si ion bombardments were performed using the Center for Irradiation Materials' Pelletron ion beam accelerator to form quantum dots and/or quantum clusters in the multinanolayer superlattice thin films to decrease the cross-plane thermal conductivity and increase the cross-plane Seebeck coefficient and cross-plane electrical conductivity. The thermoelectric and transport properties have been characterized for SiO_2/SiO_2 + Ge superlattice thin films.

Keywords

Ion bombardment, thermoelectric properties, transport properties, multinanolayers, figure of merit

Introduction

Thermoelectric materials have important applications such as waste heat transfer to electric power and solid-state Peltier coolers (Lu et al., 2010). The growing concern over increasing energy cost and global warming associated with fossil fuel sources has stimulated the search for cleaner, more sustainable energy sources (Hayakawa et al., 2011; Xiao et al., 2008). The efficiency of thermoelectric generator highly depends on the operating temperatures, the figure of merit, and design configuration including the external load parameter of the device (Sahin and Yilbas, 2013). Recent years have witnessed remarkable growing interest in thermoelectric nanocomposite for energy conversion application. One factor driving the current interest in nanocomposite thermoelectric study is needed for safe, clean, and sustainable energy source. The crisis at the Fukushima Daiichi nuclear plant due to an earthquake evoked a worldwide redraft of national future energy strategy. In March 2011, the German government stated that all reactors operational before 1980 in Germany would be taken off-line (Liu et al., 2011). Even though two basic types of nuclear power supplies have been used in space nuclear reactors and radioisotope sources in the past. In a space nuclear reactor

system, the energy source is the heat generated by the controlled fission of uranium. This heat is transferred by a heat-exchange coolant to either a static (e.g. thermoelectric) or dynamic (e.g. turbine/alternator) conversion system, which transforms it into electricity (Aftergood, 1989). The theory of thermoelectric power generation and thermoelectric refrigeration was first presented by Altenkirch in 1990 (Xi et al., 2007). Although thermoelectrics (TE) as a physical phenomenon has been known for 190 years, there are still no well-established, widespread TE applications for power

[1]Department of Electrical Engineering and Computer Science, Alabama A&M University, Normal, AL, USA
[2]NASA Marshall Space Flight Center, Huntsville, AL, USA
[3]Center for Irradiation of Materials (CIM), Alabama A&M University, Normal, AL, USA
[4]Cygnus Scientific Services, Huntsville, AL, USA
[5]Department of Physics, Alabama A&M University, Normal, AL, USA
[6]Department of Chemistry and Physics, Fayetteville State University, Fayetteville, NC, USA

Corresponding author:
Satilmis Budak, Department of Electrical Engineering and Computer Science, Alabama A&M University, 4900 Meridian Street, P.O. BOX 1955, Normal, AL 35762, USA.
Email: satilmis.budak@aamu.edu

generation in households or industry. Intensive research into materials aimed at improving thermoelectric performance and providing cost and environmental benefits has been triggered off particularly by advances in nanostructuring of semi-conducting materials. The use of waste heat from mobile and stationary energy conversion processes to optimize power generation (cars: substitution of the alternator; power plants and combined heat and power production: power production plus) and to optimize combustion in simple wood stoves (electric-driven fans for air supply) is considered promising fields of application (Patyk, 2013). For this purpose, oxide materials are potential candidates for a wide range of high-temperature applications due to their high chemical stability and the absence of harmful elements in their compositions (Bhaskar et al., 2013). The efficiency of the thermoelectric devices is limited by the material properties of n-type and p-type semiconductors (Scales, 2002). The best thermoelectric materials were succinctly summarized as "phonon-glass electron-crystal," which means that the materials should have a low lattice thermal conductivity as in glass and high electrical conductivity as in crystals (Slack, 1995). The efficiency of the thermoelectric devices is determined by the figure of merit ZT (Guner et al., 2008). The figure of merit is defined by $ZT = S^2\sigma T/\kappa$, where S is the Seebeck coefficient, σ is the electrical conductivity, T is the absolute temperature, and κ is the thermal conductivity (Huang et al., 2005). ZT can be increased by increasing S, by increasing σ, or by decreasing κ. In order to compete with conventional refrigerators, a ZT of 3 is required. Due to their limited energy conversion efficiencies (i.e. ZT is ~1), thermoelectric devices currently have a rather narrow set of applications. However, there is a reinvigorated interest in the field of TE due to classical and quantum mechanical size effects, which provide additional ways to enhance energy conversion efficiencies in nanostructured materials (Xiao et al., 2008). Semiconductor quantum dots (QDs) are a subject of intense research in the field of micro- and optoelectronics. One of the most motivating challenges is the realization of Si-based systems like Ge/Si quantum structures, which are compatible with Si-based electronic processing. Electronic and optical properties are expected to result from the three-dimensional (3D) charge carrier confinement in the islands and the zero-dimensional (0D) density of states (Fonseca et al., 2006). Phonon-grain boundary scattering has a significant effect in reducing the lattice thermal conductivity of semiconductor alloys when the phonon mean free path or wavelength is comparable to the grain size dimensions without affecting Seebeck coefficient and electrical conductivity (Dughaish, 2002). Understanding the thermal conductivity and heat transfer processes in thin films and superlattice structures is critical for the development of microelectronic

and optoelectronic devices and low-dimensional thermoelectric and thermionic devices. Experimental results on the thermal conductivity of superlattices have demonstrated that the thermal conductivity of a superlattice could be much lower than that estimated from the bulk values of its constituent materials and even smaller than the thermal conductivity values of the equivalent composition alloys (Tasciuc et al., 2000). Over the last two decades, a lot of research has been dedicated to studying the quantum-confined electronic states in low-dimension structures of group IV semiconductors like Ge. Nanocrystals (NCs) of indirect-gap semiconductors, such as Si and Ge, are widely studied, as they would open new possibilities for the application of these materials in novel integrated optoelectronics and microelectronics devices. Several techniques are being used to fabricate Ge NCs, such as radio frequency (RF) co-sputtering, direct current (DC) sputtering, ion implantation, evaporation–condensation, electron beam evaporation, chemical vapor deposition, and pulsed laser deposition (Caldelas et al., 2008). In this study, we report on the growth of SiO_2/SiO_2 + Ge multilayer superlattice thin film systems using ion beam–assisted deposition (IBAD) followed by high-energy Si ions bombardment of the films for reducing the cross-plane thermal conductivity and increasing the cross-plane electrical conductivity and cross-plane Seebeck coefficients due to the nanodots and/or nanocluster effects during the MeV Si ion bombardments, X-ray photoelectron spectroscopy (XPS), Van der Pauw resistivity, mobility and Hall Effect coefficient measurements.

Experimental

We have deposited the 100 alternating nanolayers of SiO_2/SiO_2 + Ge thin films on silicon and fused silica (Suprasil) substrates with IBAD. The IBAD system was used as a physical vapor deposition (PVD) system since we have used only two electron guns to evaporate the crucibles without any gas assistance. The multinanolayered thin films were sequentially deposited to have a periodic structure consisting of alternating SiO_2 and SiO_2 + Ge layers. These thin films form a periodic quantum well (QW) structure consisting of 100 alternating layers of total thickness of 190 nm. The deposited multilayer films have an alternating layer of about 1.9 nm thick. The two electron-gun (e-guns) evaporators for evaporating the two solids were turned on, and shutter for Ge crucible was turned on and off alternately to form SiO_2 and SiO_2 + Ge multilayers. The base pressure obtained in IBAD chamber was about 5×10^{-6} Torr during the deposition. The current for the e-guns during the deposition was about 45 mA for SiO_2 (fused silica) and 30 mA for Ge crucibles. The growth rate was monitored by INFICON Quartz
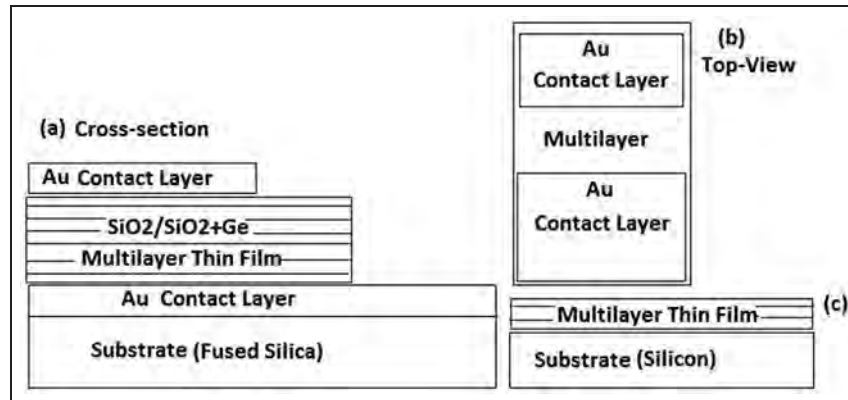
Figure 1. Geometries of the samples from (a) the cross section and (b) the top view for the cross plane Seebeck and the cross plane electrical conductivity and (c) the cross section for the cross plane thermal conductivity and in plane electrical conductivity measurements.

Crystal Microbalance (QCM). Figure 1 shows the geometries of the samples from (a) the cross section and (b) the top view for the cross-plane Seebeck and the cross-plane electrical conductivity and (c) the cross section for the cross-plane thermal conductivity and in-plane electrical conductivity measurement.

The cross-plane electrical conductivity was measured by the Agilent four-probe micro-ohmmeter contact system; in-plane electrical conductivity, mobility, and Hall Effect coefficient measurements were performed by MMR Technologies Van der Pauw and Hall Effect measurement system; and the thermal conductivity was measured by the home-made 3ω (third harmonic) technique. The cross-plane electrical conductivity, thermal conductivity and Seebeck coefficient measurements have been performed at the room temperature. Detailed information about the 3ω (third harmonic) technique may be found in Holland and Smith (1966), Cahill et al. (1994), and Tasciuc et al. (2001). In order to make nanostructures (nanodots and/or nanoclusters) in the layers, 5 MeV Si ion bombardments were performed with the Pelletron ion beam accelerator at Center for Irradiation of Materials (CIM). The energy of the bombarding Si ions was chosen by the SRIM simulation software. The fluences used for the bombardment were between 1×10^{12} ions cm^{-2} and 1×10^{14} ions cm^{-2}. The XPS spectra were measured by STAIB Multichannel Analysis System.

Results and discussion

The thickness of 100 alternating nanolayers of SiO$_2$/SiO$_2$ + Ge thin film was found to be 190 ($\pm$10) nm using Fabry–Pérot optical interferometer. Figure 1 shows the geometries of the samples from (a) the cross section and the top view for the cross-plane Seebeck and the cross-plane electrical conductivity, and (c) the cross section for the cross-plane thermal conductivity
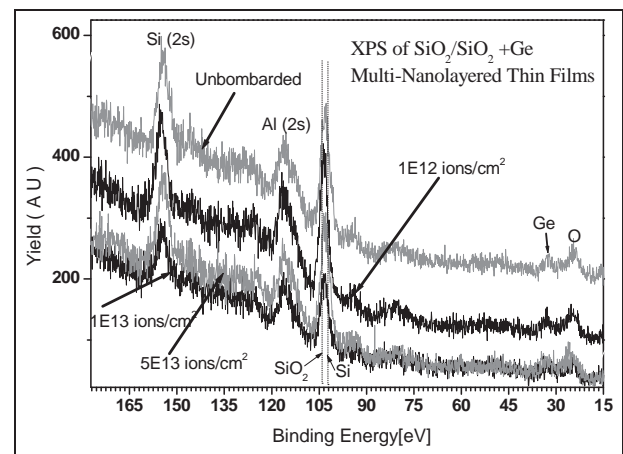

Figure 2. XPS spectra of SiO$_2$/SiO$_2$ + Ge multinanolayered thin films at different fluences.
XPS: X-ray photoelectron spectroscopy.

and in-plane electrical conductivity measurement. The thin films of SiO$_2$/SiO$_2$ + Ge were deposited on the fused silica and silicon substrates. The silica and silicon-deposited thin films have been used for the thermal, electrical, and optical measurements. Figure 2 shows XPS spectra of SiO$_2$/SiO$_2$ + Ge multinanolayered thin films at different fluences at different binding energies between 175 and 15 eV. As seen from Figure 2, each element has its own XPS peak at different binding energy levels in the whole XPS spectrum for each film. Oxygen (O) has the peak at the binding energy of 15 eV, Ge has the peak at the binding energy of 35 eV, and Si has the peak at the binding energy of 155 eV. We have seen a peak belong to Al in the XPS spectra even we did not use Al during the deposition. The reason might be the contamination from one of our previous depositions. The intensities of the peaks for all unbombarded and high energy bombarded samples at the different fluences look almost the same except for the intensity at

the fluence of 1×10^{13} ions cm^{-2}. The amplitudes of the peaks for each element used in the deposition got smaller at the fluence of 1×10^{12} ions cm^{-2}. When the first fluence of 1×10^{12} ions cm^{-2} was introduced, the XPS peak started to shift in the yield axis direction without almost no change in the intensities of the peaks of the each element. When the fluence was being continued to the fluence of 1×10^{13} ions cm^{-2}, the whole XPS spectrum shifted more in the negative yield axis direction. The shifting of the XPS spectrum changed in the positive yield axis direction at the fluence of 5×10^{13} ions cm^{-2}. The ion bombardment might cause Ge atoms to move and embed in the multilayers of SiO_2 + Ge. The alloy structure of SiO_2 + Ge layers might get nanodots and/or nanoclusters of Ge atoms. This could cause increment in the electrical conductivity. The movements of semiconductor Ge atoms through the multilayers might have the effects of XPS shifts. The approximate mass ratio between Si and Ge could be estimated using the area under the XPS curve as 100:5. There are many studies in the literature, which used either ion beam bombardments or temperature annealing to form NCs and or clusters in the SiO_2 or in the other dielectric matrix. They have performed optical and electrical characterizations to show the effects of the quantum confinements due to ion bombardments or temperature annealing. Some of them could be seen in Hosono et al. (1995), Caldelas et al. (2008), Djurabekova et al. (2009), Schmidt et al. (2007), Rao et al. (2007), Wu et al. (2002), and Joshi et al. (2009).

Figure 3 shows Van der Pauw sheet resistivity measurements of unbombarded and bombarded SiO_2/SiO_2 + Ge multinanolayered thin films at the temperatures between 300 and 580 K. The in-plane resistivity has the value of about 5.3 Ω cm at 300 K for the unbombarded sample. When the temperature was increased, the resistivity started to decrease and approached zero value at the temperature of about 340 K. The decrease in the resistivity for the semiconductor thin films depending on the increased temperature is one of the expected things in the semiconductor and thermoelectric material systems. The meaning of this behavior is that the electrical conductivity values of the thin film system increase while the temperature is increased from the room temperature to the higher values. After the temperature of 460 K, the resistivity started to increase for the unbombarded sample. The reason might be the more temperature effects on the material system. When the thin films were bombarded with the fluence of 5×10^{13} ions cm^{-2}, the resistivity decreased from the value of 5.3 Ω cm to about 1.2 Ω cm at 300 K. This shows that the high-energy Si ion bombardments decreased the resistivity of the thin film systems due to the nanodots and/or nanocluster formations in the multilayered thin films. This is one of the expected results of the ion beam bombardments on the thin film material system.

Figure 4 shows mobility measurements of unbombarded and bombarded SiO_2/SiO_2 + Ge multinanolayered thin films at the temperatures between 300 and 580 K. The mobility of the SiO_2/SiO_2 + Ge multinanolayered thin film has very small magnitudes in the amplitudes depending on the temperature between 300 and 580 K for the unbombarded sample. When the thin film system was bombarded with 5 MeV Si ions at the fluence of 5×10^{12} ions cm^{-2}, the mobility values show some increments at some temperatures due to the increase in the charge carrier concentration because of the Si ion bombardments. This is one of the expected results of the high-energy ion beam bombardments to increase the mobility of the thin film system. Koch and Ziemann (1997) showed that the main effect of the
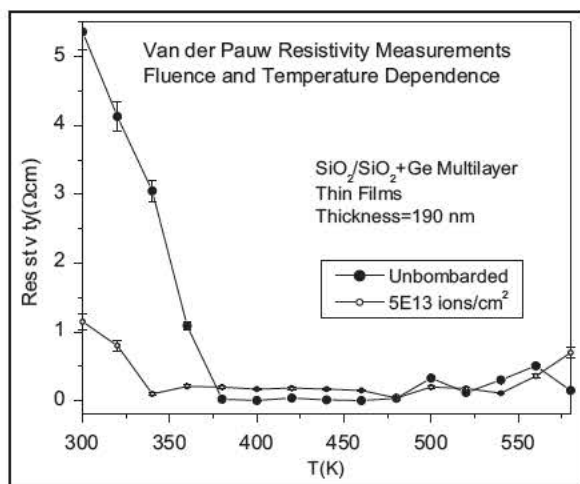

Figure 3. Van der Pauw resistivity measurements of unbombarded and bombarded SiO_2/SiO_2 + Ge multinanolayered thin films.
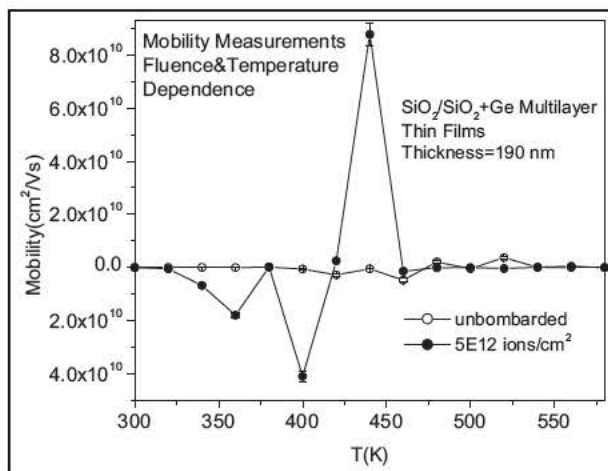

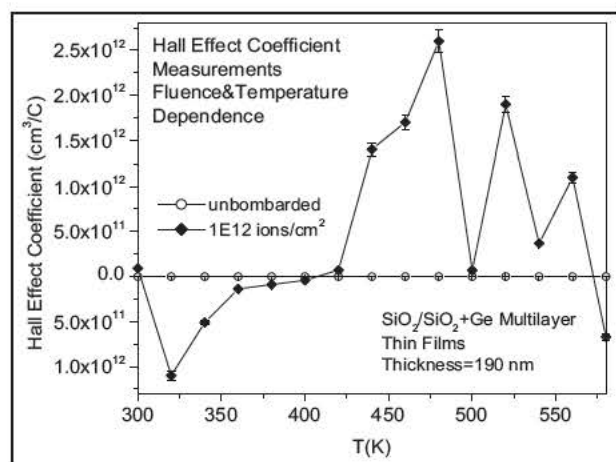**Figure 4.** Mobility measurements of unbombarded and bombarded SiO_2/SiO_2 + Ge multinanolayered thin films.

Figure 5. Hall Effect coefficient measurements of unbombarded and bombarded SiO$_2$/SiO$_2$ + Ge multinanolayered thin films.

bombardment with Ar ions is to enhance the mobility of the Zr atoms. The main effect of ion bombardment is to enhance the surface mobility of the arriving atoms rather than direct implantation. The observed transformation from an amorphous into a crystalline structure must originate from the ion-bombardment-induced local agitation. It is well known that a portion of the ion energy transmitted to the host atoms appears in the form of strong lattice vibrations, which can be equivalent to very high local temperatures on the atomic scale. This eventually leads to enhanced atomic mobility and, therefore, to a structural relaxation process, which is essential for the crystallization process (Ziebert et al., 2011).

Figure 5 shows Hall Effect coefficient measurements of unbombarded and bombarded SiO$_2$/SiO$_2$ + Ge multinanolayered thin films at the temperatures between 300 and 580 K. The Hall Effect coefficient of the SiO$_2$/SiO$_2$ + Ge multinanolayered thin film has very small magnitudes in the amplitudes depending on the temperature between 300 and 580 K for the unbombarded sample. When the thin film system was bombarded with 5 MeV Si ions at the fluence of 1×10^{12} ions cm^{-2}, the Hall Effect coefficients show some increments at some temperatures due to the increase in the charge carrier concentration because of the Si ion bombardments. The Hall Effect coefficient reached the maximum value of about 2.6×10^{12} cm^3 C^{-1} at the temperature of about 475 K and the minimum value of 0.9×10^{12} cm^3 C^{-1} at the temperature of about 320 K. High-energy Si beam showed positive effects in the Hall Effect coefficients if the suitable fluence is chosen.

Figure 6 shows thermoelectric properties of 100 alternating nanolayers of SiO$_2$/SiO$_2$ + Ge virgin (unbombarded) and 5 MeV Si ion bombarded multinanolayered thin films at six different fluences. Figure 6(a) shows the square of the Seebeck coefficient
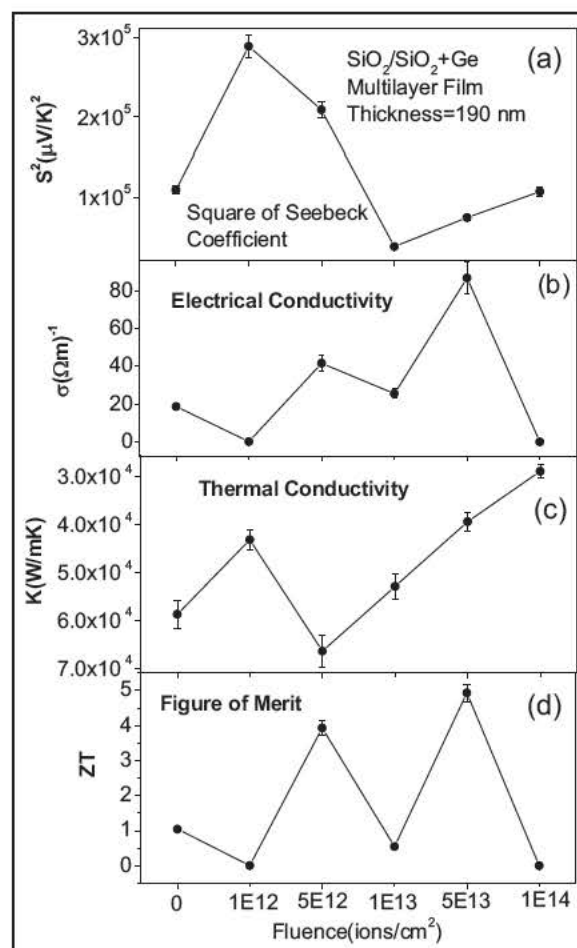

Figure 6. Thermoelectric properties of SiO$_2$/SiO$_2$ + Ge multinanolayered thin films at different fluences: (a) square of the Seebeck coefficient, (b) electrical conductivity, (c) thermal conductivity, and (d) figure of merit.

of the thin film systems at different applied high-energy fluences. The original Seebeck values are negative. This shows that we have negative thermopower and electrons are the main charge carriers. The virgin sample has the Seebeck coefficient of -330.41 μV K^{-1} at the room temperature, and this value increased to a maximum value of -537.22 μV K^{-1} at the fluence of 1×10^{12} ions cm^{-2}. Seebeck coefficient reached the minimum value of -193.93 μV K^{-1} at the fluence of 1×10^{13} ions cm^{-2}. This material system showed very high thermopower values due to the effect of high-energy Si ion beam bombardments.

Figure 6(b) shows the electrical conductivity values calculated from the Van der Pauw sheet resistivity measurements of SiO$_2$/SiO$_2$ + Ge multinanolayered thin films at the six different applied fluences including zero fluence (unbombarded). As seen from Figure 6(b), the electrical conductivity values increased at the fluences of 5×10^{12} ions cm^{-2} and 5×10^{13} ions cm^{-2}. The other fluences showed decrease in the electrical conductivity

values. The maximum value of the electrical conductivity of 87 $(\Omega \text{ m})^{-1}$ was reached at the fluence of 5×10^{13} ions cm^{-2}. This shows that the MeV Si ion bombardments show positive effects in the electrical conductivity at the suitable fluences. The increase in the electrical conductivity is one of the expected values for the high-efficient thermoelectric materials and devices. Enhancement of the Seebeck coefficient without reducing the electrical conductivity is essential to realize practical thermoelectric materials exhibiting a dimensionless figure of merit exceeding 2. Ohta et al. (2007) demonstrated that a high-density two-dimensional electron gas confined within a unit cell layer thickness in SrTiO$_3$ yields unusually large, approximately five times larger than that of SrTiO$_3$ bulks, while maintaining a high electrical conductivity. There are many studies in the literature working on the Ge-embedded silica matrix systems. The bulk electrical conductivity value shows us how the nanolayered system works more efficiently in increment of the electrical conductivity. Germanium has the electrical conductivity of 2.17 (S m^{-1}) at about room temperature (Griffiths, 1999 [1981]; Serway, 1998). The bulk electrical conductivity of the fused silica is also given as 1.3×10^{-18} S m^{-1} (Serway, 1998). The electrical conductivity which we calculated from the sheet resistance of SiO$_2$/SiO$_2$ + Ge multilayer thin films starts from 20 S m^{-1} and reached 80 S m^{-1} depending on the used fluence of the high-energy ion bombardment as shown in Figure 6(b). This shows that the nanolayered thin film structures have shown very improved electrical properties of the material systems with respect to their bulk properties (Ohta et al., 2007). Electrons (or holes) and phonons have two length scales associated with their transport, wavelength, and mean free path. By nanostructuring semiconductors with sizes comparable to the wavelength, sharp edges and peaks in their electronic density of states are produced, whose location in energy space depends on size. By matching the peak locations and shape with respect to the Fermi energy, one could tailor the Seebeck coefficient. Furthermore, such quantum confinement also increases electronic mobility, which could lead to high values of the electrical conductivity. Hence, quantum confinement allows manipulation of the Seebeck coefficient square times the electrical conductivity (Majumdar, 2004).

Figure 6(c) shows the cross-plane thermal conductivity change depending on the applied six different fluences of 5 MeV Si ion beam bombardments. As shown in Figure 6(c), the thermal conductivity value increased and decreased at different fluences. The minimum value of the thermal conductivity was reached at the fluence of 5×10^{12} ions cm^{-2}. The ion beam bombardments did not show more positive effects on the cross-plane thermal conductivity values since the more high-energy beam might have destroyed the multinanolayered

superlattice thin film structures. Tasciuc et al. (2000) used the 3ω technique to measure the cross-plane thermal conductivity of the symmetrically strained Si/Ge superlattices. Their thermal conductivity values varied from 2.9 to 4.0 W m^{-1} K^{-1} at room temperature. The room-temperature thermal conductivity of as-grown polycrystalline silicon is found to be 13 W m^{-1} K^{-1} and that of amorphous recrystallized polycrystalline silicon is 22 W m^{-1} K^{-1}, which is almost an order of magnitude less than that of single-crystal silicon (Uma et al., 2001). Neither Si nor Ge is a good TE material, as the lattice thermal conductivity is very large (150 W m^{-1} K^{-1} for Si and 63 W m^{-1} K^{-1} for Ge). The lattice thermal conductivity can be substantially reduced by alloy formation between the two elements (Tritt and Subramanian, 2006). In our superlattice system, we have prepared the SiO$_2$/SiO$_2$ + Ge amorphous multilayer films. Our cross-plane thermal conductivity values take the values between 2.89×10^{-4} and 6.64×10^{-4} W m^{-1} K^{-1} at room temperature at different applied ion beam fluences. Our results are much smaller than what Tasciuc et al. (2000) found, even ion beam bombardments did not show very positive effects in our thin film systems. The reason for the low thermal conductivity might be due to the fact that the high-energy Si ion bombardments form nanodots and/or nanoclusters in the multilayer thin films, these formations cause phonon scattering and quantum confinement in the multilayer thin film systems to cause a reduction in the cross-plane thermal conductivity. Balandin and Wang (1998) studied the effects of phonon spatial confinement and showed that the thermoelectric figure of merit is strongly enhanced in QWs and superlattices due to two-dimensional carrier confinement. Figure 6(d) shows the calculated dimensionless figure of merit ZT values by applying the equation given in the "Introduction" section. These multilayered thin film systems showed very high figure of merit even it is very hard to find in the literatures. Even before it was bombarded, the ZT value was 1.04. When these materials have been bombarded, the better values of the figure of merits have been reached. The maximum results of ion bombardment on ZT strongly appeared as 3.93 at the fluence of 5×10^{12} ions cm^{-2} and as 4.93 at the fluence of 5×10^{13} ions cm^{-2}.

Conclusion

We have grown 100 periodic nanolayers of SiO$_2$/SiO$_2$ + Ge superlattice thin films on the silicon and fused silica substrates (Suprasil) at the total thickness of 190 nm using IBAD. The multilayer films were sequentially deposited to have a periodic structure consisting of alternating SiO$_2$ and SiO$_2$ + Ge layers. The deposited multilayer films have an alternating layer of about 1.9 nm thick.

Some optical properties like XPS; transport properties like electrical conductivity, mobility, and Hall Effect coefficients; thermoelectrical properties like Seebeck coefficient, electrical conductivities, and thermal conductivities have been studied to characterize the multinanolayered thin film systems. XPS spectra of SiO_2/SiO_2 + Ge multinanolayered thin films have been gathered at different fluences at different binding energies between 175 and 15 eV. Van der Pauw resistivity, mobility, and Hall Effect coefficients have been investigated at five different fluences in addition to the unbombarded sample at different temperatures between 300 and 580 K. Some meaningful data were collected for the suitable fluences for the optical and transport properties as of the effect of the ion beam bombardments on the multilayered thin film systems. The maximum value of Seebeck coefficient of 537.22 μV K^{-1} was reached at the fluence of 1×10^{12} ions cm^{-2}. The maximum value of the electrical conductivity of 87 (Ω m)$^{-1}$ was reached at the fluence of 5×10^{13} ions cm^{-2}. Cross-plane thermal conductivity values take the values between 2.89×10^{-4} and 6.64×10^{-4} W m^{-1} K^{-1} at room temperature at different applied ion beam fluences. The maximum figure of merit value of about 4.93 has been reached at the fluence of 5×10^{13} ions cm^{-2}. This result is very remarkable for the room-temperature characterizations for the materials among the thermoelectric material systems. The high-energy ion bombardment can produce nanostructures and modify the property of thin films (Budak et al., 2007), resulting in lower thermal conductivity and higher electrical conductivity at the suitable energy and fluences.

References

Aftergood S (1989) Background on space nuclear power. *Science and Global Security* I: 93 107.

Balandin A and Wang KL (1998) Effect of phonon confinement on the thermoelectric figure of merit of quantum wells. *Journal of Applied Physics* 84: 6149.

Bhaskar A, Liu C J, Yuan JJ, et al. (2013) Thermoelectric properties of n type Ca$_{1-x}$BixMn$_{1-y}$SiyO$_{3-d}$ (x = y = 0.00, 0.02, 0.03, 0.04, and 0.05) system. *Journal of Alloys and Compounds* 552: 236 239.

Budak S, Muntele C, Zheng B, et al. (2007) MeV Si ions bombardment effects on thermoelectric properties of sequentially deposited SiO_2/Au$_x$SiO$_{2(1-x)}$ nano layers. *Nuclear Instruments & Methods in Physics Research Section B: Beam Interactions with Materials and Atoms* 261: 1167.

Cahill DG, Katiyar MJ and Abelson R (1994) Thermal conductivity of a Si:H thin films. *Physical Review B* 50: 6077.

Caldelas PA, Rolo G, Gomes MJM, et al. (2008) Raman and XRD studies of Ge nanocrystals in alumina films grown by RF magnetron sputtering. *Vacuum* 82: 1466 1469.

Djurabekova F, Backmana M, Pakarinen OH, et al. (2009) Amorphization of Ge nanocrystals embedded in amorphous silica under ion irradiation. *Nuclear Instruments & Methods in Physics Research Section B: Beam Interactions with Materials and Atoms* 267: 1235 1238.

Dughaish ZH (2002) Lead telluride as a thermoelectric material for thermoelectric power generation. *Physica B* 322: 205.

Fonseca A, Alves E, Barradas NP, et al. (2006) RBS/channeling study of buried Ge quantum dots grown in a Si layer. *Nuclear Instruments & Methods in Physics Research Section B: Beam Interactions with Materials and Atoms* 249: 462 465.

Griffiths D (1999 [1981]) Electrodynamics. In: Reeves A (ed.) *Introduction to Electrodynamics*. 3rd ed. Upper Saddle River, NJ: Prentice Hall, p. 286.

Guner S, Budak S, Minamisawa RA, et al. (2008) Thickness and MeV Si ions bombardment effects on the thermoelectric properties of Ce$_3$Sb$_{10}$ thin films. *Nuclear Instruments & Methods in Physics Research Section B: Beam Interactions with Materials and Atoms*. 266: 1261.

Hayakawa Y, Arivanandhan M, Saito Y, et al. (2011) Growth of homogeneous polycrystalline Si$_{1-x}$Ge and Mg$_2$Si$_{1-x}$Gex for thermoelectric application. *Thin Solid Films* 519: 8532 8537.

Holland LR and Smith RC (1966) Analysis of temperature fluctuations in ac heated filaments. *Journal of Applied Physics* 37: 4528.

Hosono H, Ueda N, Kawazoe H, et al. (1995) Optical and electrical properties of proton implanted amorphous SiO2, GeO2 SiO 2, MgO P205 and nanocrystalline MgIn204: novel materials by proton implantation. *Journal of Non Crystalline Solids* 182: 109 118.

Joshi KU, Narsale AM, Kanjilal D, et al. (2009) Ion beam synthesis of germanium nanostructures. *Surface & Coatings Technology* 203: 2476 2478.

Koch T and Ziemann P (1997) Effects of ion beam assisted deposition on the growth of zirconia films. *Thin Solid Films* 303: 122 127.

Liu W, Yanm X, Chen G, et al. (2011) Recent advances in thermoelectric nanocomposites. *Nano Energy*. DOI: 10.1016/j.nanoen.2011.10.001.

Lu P X, Wu F, Han H L, et al. (2010) Thermoelectric properties of rare earths filled CoSb$_3$ based nanostructure skutterudite. *Journal of Alloys and Compounds* 505: 255 258.

Majumdar A (2004) Thermoelectricity in semiconductor nanostructures. *Science* 303: 777.

Ohta H, Kim S, Mune Y, et al. (2007) Giant thermoelectric Seebeck coefficient of a two dimensional electron gas in SrTiO$_3$. *Nature Materials* 6: 129.

Patyk A (2013) Thermoelectric generators for efficiency improvement of power generation by motor generators environmental and economic perspectives. *Applied Energy* 102: 1448 1457.

Rao N, Srinivasa DS, Pathak AP, et al. (2007) Structural studies of Ge nanocrystals embedded in SiO$_2$ matrix. *Nuclear Instruments & Methods in Physics Research Section B: Beam Interactions with Materials and Atoms* 264: 249 253.

Sahin AZ and Yilbas BS (2013) The thermoelement as thermoelectric power generator: effect of leg geometry on the efficiency and power generation. *Energy Conversion and Management* 65: 26 32.

Scales BC (2002) Smaller is cooler. *Science* 295: 1248.

Schmidt B, Mucklich A, Rontzsch L, et al. (2007) How do high energy heavy ions shape Ge nanoparticles embedded in SiO$_2$? *Nuclear Instruments & Methods in Physics Research Section B: Beam Interactions with Materials and Atoms* 257: 30 32.

Serway RA (1998) *Principles of Physics*. 2nd ed. Fort Worth, TX; London: Saunders College Pub, p. 602.

Slack G (1995) New materials and performance limits for thermoelectric cooling. In: Rowe DM (ed.) *CRC Handbook of Thermoelectrics*. CRC Press, LLC, Boca Raton, FL, p. 407.

Tasciuc TB, Kumar AR and Chen G (2001) Data reduction in 3ω method for thin film thermal conductivity determination. *Review of Scientific Instruments* 72: 2139.

Tasciuc TB, Liu W, Liu J, et al. (2000) Thermal conductivity of symmetrically strained Si/Ge superlattices. *Superlattices and Microstructures* 28: 199.

Tritt TM and Subramanian MA (2006) Thermoelectric materials, phenomena, and applications: a bird's eye view. *MRS Bulletin* 31: 188 198.

Uma S, McConnell AD, Asheghi K, et al. (2001) Temperature dependent thermal conductivity of undoped polycrystalline silicon layers. *International Journal of Thermophysics* 22(2): 605 616.

Wu XM, Lu MJ and Yao WG (2002) Structure and optical properties of SiO2 films containing Ge nanocrystallites. *Surface & Coatings Technology* 161: 92 95.

Xiao F, Hangarter C, Yoo B, et al. (2008) Recent progress in electrodeposition of thermoelectric thin films and nanostructures. *Electrochimica Acta* 53: 8103 8117.

Xi H, Luo L and Fraisse G (2007) Development and applications of solar based thermoelectric technologies. *Renewable & Sustainable Energy Reviews* 11: 923 936.

Yoo BY, Huang C K, Lim JR, et al. (2005) Electrochemically deposited thermoelectric n type Bi$_2$Te$_3$ thin films. *Electrochimica Acta* 50: 4371.

Ziebert C, Ye J, Stüber M, et al. (2011) Ion bombardment induced nanocrystallization of magnetron sputtered chromium carbide thin films. *Surface & Coatings Technology* 205: 4844 4849.